2004

Conceptual Design Study of a Supersonic Compressor Applied to Refrigerant Compression Cycles

Shawn P. Lawlor
Ramgen Power Systems

Paul M. Brown
Ramgen Power Systems

Steven G. Mackin
Ramgen Power Systems

CONCEPTUAL DESIGN STUDY OF A SUPERSONIC COMPRESSOR APPLIED TO REFRIGERANT COMPRESSION CYCLES

Shawn P. Lawlor, Paul M. Brown, Steven G. Mackin

Ramgen Power Systems
Bellevue, Washington, USA
(425) 828-4919

ABSTRACT

A family of innovative high performance supersonic compressors has been proposed. These compressors combine many of the aspects of shock compression systems commonly used in supersonic flight inlet design in conjunction with turbo-machinery design practices employed in conventional axial and centrifugal compressor design. The result is a high efficiency compressor that is capable of single stage pressure ratios of up to 10:1. A variety of design configurations for land-based compressors utilizing this system have been explored. Preliminary demonstration testing of one such air compressor rotor has recently been completed.

It is anticipated that a family of compressors capable of operating on a wide range of process and/or refrigeration gases could be developed using the supersonic inlet shock compression technology. The basic principals of operation of the shock compression stage are presented along with selected data from initial testing. Finally, using the design practices and tools developed over the course of the rig design and test effort, six conceptual refrigerant compressor systems were defined and evaluated.

1. INTRODUCTION

A prototype version of a supersonic compression system has been designed, developed and tested. This system applies supersonic aerodynamics design practices that are common in flight propulsion applications to the land based compression of a working gas. The result is an axial flow supersonic compression stage with uniquely low blade counts and shallow blade angles. An additional feature seldom applied in either axial or centrifugal stages is the use of "on-rotor" boundary layer bleed for gas path starting and performance optimization. This technique, referred to by some compressor designers as aspiration (Kerrebrock *et al.*, 1998), has been proposed as a method for minimizing shock-boundary layer interactions and associated boundary layer separation and was included in the design of the supersonic rotor tested here.

A proof-of-concept system has been designed to demonstrate the basic operational characteristics of this family of compressors when operating on air. The test unit was designed to process ~1.43 kg/s and to produce a pressure ratio across the supersonic rotor of 2.25:1. While the primary goal of these compressor tests has been to prove the basic design for application to higher pressure ratio air compression applications, the pressure ratios already demonstrated on air would be of particular interest in a number of refrigeration compression applications.

This paper will present the basic theory of operation of the proposed compression process, highlight preliminary test results from recent rig tests using air as a working fluid and then present and explore the conceptual design of some basic refrigeration compression systems of interest for current applications.

2. THEORY OF OPERATION

While supersonic axial compressor stages have been suggested by a number of other investigators (Kantrowitz, 1946, Wright and Klapproth, 1949, Jacklitch and Hartman, 1953, Wilcox *et al.,* 1959, Simon, 1973) those rotor stages have invariably been configured so as to resemble conventional axial flow rotors. They have relatively high blade counts and shock systems generated by the blade surfaces. In the case of the present rotor, the configuration was developed with an oblique shock system and terminal normal shock using the design guidelines typically

employed in supersonic flight inlet design. Downstream of the normal shock, the flow is subsonic with a Mach number of ~0.8. Following the normal shock a planar diffuser brings the flow to a Mach number of ~0.5 as it leaves the rotor.

The rotor flow-path is formed by three elongated blades or strakes mounted on the rim of the rotor. These strakes are mounted on the rotor at a shallow blade angle of 5°-10° and form the axial boundaries of each of the three flow-paths as shown in Figure 1. The shock system is generated by a ramp integrated into the rim of the rotor and reflected off the non-rotating compressor case as shown in the lower illustration of Figure 2. The pattern of shock waves is comparable to the pattern of shock waves that might be found in a supersonic inlet as would be applied to a missile or supersonic aircraft. This comparison is represented by the upper illustration in Figure 2.

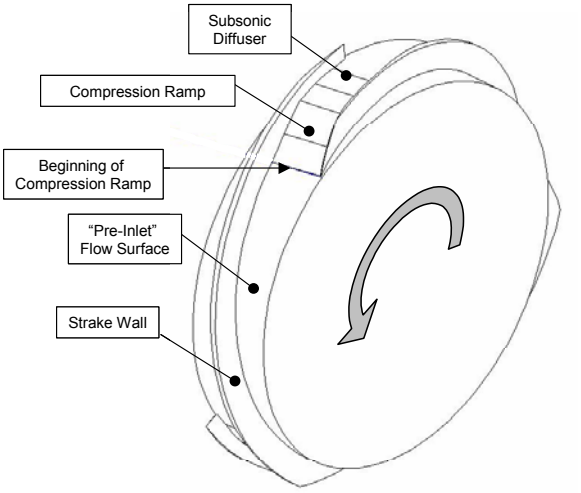

Figure 1. Supersonic compression stage rotor

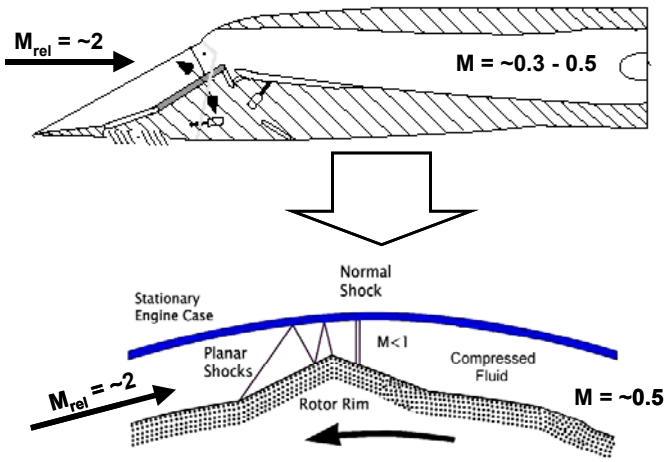

Figure 2. Shock structure & comparison to flight inlet

Table 1. Rotor Inflow Conditions

Rotor Speed	***(rpm)***	21,100
Shroud Radius	***(cm)***	14.51
Rim Radius	***(cm)***	12.78
Mass Flow	***(kg/s)***	1.43

Reference Frame / ***Property***		***Inertial Reference Frame***	***Relative Reference Frame***
T	***(K)***	260	260
ρ	***(kg/m^3)***	1.312	1.312
M	***(---)***	0.70	1.61
V	***(m/s)***	225.9	225.9
V_{axial}	***(m/s)***	68.9	68.9
V_{tan}	***(m/s)***	215.1	215.1
P_t	***(kPa)***	145.14	430.32
T_t	***(K)***	287	398

The combination of the strakes, rotor rim and non-rotating case form a rectangular flow-path with an inflow Mach number that is determined by the rotation rate of the rotor and any pre-swirl that is imparted into the flow upstream of the rotor. In the present case, the design rotor speed was 21,100 rpm. The combination of the rotor speed and the pre-swirl from the upstream cascade of nozzles created a rotor inflow that was supersonic relative to the moving rotor. The details of the flow-field are summarized in Table 1.

In the case of a supersonic inlet for flight applications, the total pressure available in the approaching stream-tube can be expressed in terms of the approach Mach number (relative to the inlet) by the familiar expression.

$$P_t = P(1+\frac{\gamma-1}{2}M_0^2)^{\frac{\gamma}{\gamma-1}} \qquad (1)$$

For inlet relative Mach numbers ranging from 1.5 to 3.5 it is common practice to design the inlet so as to establish a series of oblique shock waves that decelerate the supersonic flow entering the inlet inflow plane from the inlet relative Mach number to a pre-normal shock Mach number of ~1.3. The losses of these shock systems are functions of the inflow Mach numbers and the turning angles

associated with each shock wave. Over the years rough guidelines have emerged to quantify the anticipated losses of such supersonic inlets for operation at various Mach numbers (Billig and Van Wie, 1987). Losses for such inlets are often expressed in terms of total pressure recovery π_{Pt}. The total pressure recovery is a commonly used inlet performance metric that is used when the temperature increases resulting from the compression process are low enough that the gas can be considered as ideal and calorically perfect throughout the process (constant γ). When a calorically imperfect or non-ideal gas is considered, it becomes important to use a performance metric that properly accounts for the changes in gas properties through the compression process.

The following relations show conservative guidelines for flight inlet performance levels in terms π_{Pt} for military and aircraft industry inlet systems.

$$\pi_{Pt} = 1 - 0.075(M_0 - 1)^{1.35} \quad (2)$$

$$\pi_{Pt} = 1 - 0.1(M_0 - 1)^{1.5} \quad (3)$$

Equations 1, 2 and 3 are shown in Figure 3 along with measured performance levels for a range of flight inlets (solid triangles). These relations should be viewed as general guidelines only and are strongly influenced by the mission requirements for the associated flight systems. Stable operation over a wide flight Mach number range as well as roll, pitch and yaw attitudes can impose serious performance penalties on a flight system. For any given operating Mach number, superior performance can be achieved by optimizing a design for operation at a single inlet relative Mach number with no significant inflow perturbations. Point A in Figure 3 is a representative data point for a mixed compression inlet designed for operation at a flight Mach number of 2.70 and illustrates the margin for improvement that is available when a design is optimized for a given operating condition.

To put the compression process efficiency implications of Figure 3 into perspective, consider the Point A. At a flight Mach number of 2.7 the stream tube captured by the inlet would have a total pressure (due to its relative Mach number) of Approximately 26 times the free stream static pressure. When tested at a relative Mach number of 2.7, the inlet discussed in NASA TM-106728 achieved a total pressure recovery of 0.91. Thus, using a combination of oblique and normal shock waves the inlet was able to recover 91% of the total pressure in the captured stream tube while decelerating the flow from a Mach number of 2.7 to 0.5. The inlet alone achieved a compression ratio of 23:1 based on static pressures.

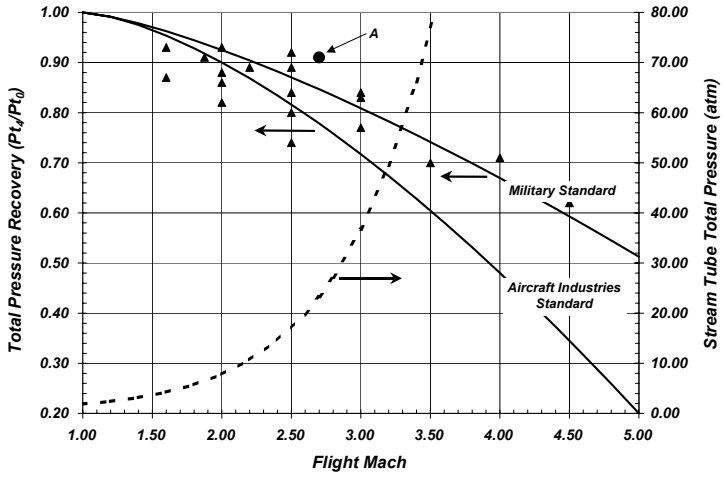

Figure 3. Flight inlet performance characteristics

Figure 4 shows the overall compression ratio that would result from "Military Standard" performance levels illustrated in Figure 3 and also expresses the efficiency of the shock compression process in terms of adiabatic compression efficiency, η_{ad}, which is a performance metric commonly used by axial and centrifugal compressor designers. The adiabatic efficiency levels shown in Figure 4 for Point A and the "Military Standard" performance trend do not include any of the pre-swirl, de-swirl or diffusion losses typically associated with the stator elements in a ground based axial or centrifugal compressor.

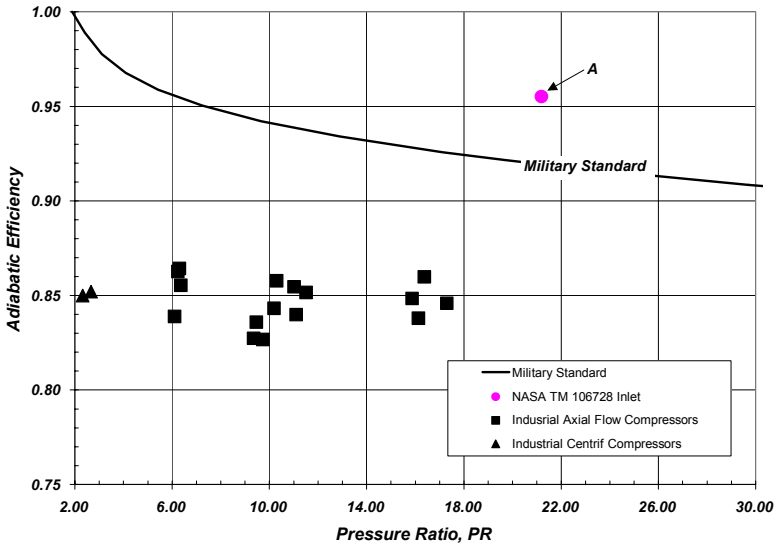

Figure 4. Flight inlet performance in terms of η_{ad}

Figure 4 shows that when properly designed, supersonic flight inlets can deliver compression ratios ranging from 2.0:1 to 30:1 depending on flight Mach number and total pressure recovery. Moreover, if the efficiency levels indicated in Figure 4 for flight inlet systems could be achieved in a ground based compression system, such a system would achieve peak efficiency levels superior to many conventional (axial & centrifugal) compression systems operating at comparable pressure ratios. To illustrate this point, the performance levels for a number of axial flow compressors used on industrial gas turbines (solid squares) have been plotted on Figure 4 as well as a few performance points for lower pressure ratio centrifugal stages used in existing multi-stage inter-cooled air turbo-compressor systems.

3. SUMMARY OF RIG TEST RESULTS

The intent of the current test rig was to validate the design methodology and predictive tools used to design this type of compression system. In addition, the performance and stability of the supersonic shock compression system was to be investigated. No effort was made to optimize the performance of the pre-swirl system or recover any of the pressure in the high swirl rotor discharge flow. As a result, all of the presented performance levels and measurements relate to the property changes across the supersonic rotor only.

There are a number of areas that require special attention in the design of this system. Understanding the sensitivity of the system to these issues was a high priority in the test program. The pressure ratio of this stage is high compared to most axial flow stages. As a result, the potential for tip leakage from the high pressure side of the strake to the low pressure side to disrupt the flow-field in the relatively long pre-inlet section leading into the shock compression ramp is an area of particular concern. Attempts were made to characterize these losses using numerical simulations as well are more simplified analytical models. The resulting loss levels were included in the performance model.

The test rig included a thermally controlled tip clearance control ring. The inside diameter of the ring was coated with an abradable material that was intended to be rubbed by the strake tips to achieve the smallest possible tip gap and therefore minimize tip leakage. The tip ring was heated, generating a relatively large tip gap, during the starting process and then cooled using cryogenic N_2 to minimize the tip gap when at full speed. One clear result of the test program was that the performance was highly dependant on tip gap and tip leakage. A complicating factor was the surface finish of the rubbed abradable surface. The combination of the strake tip speed, incursion rate and abradable composition resulted in a surface finish that increased tip leak rates compared to a tip gap with a smooth finish on the non-rotating case.

Another area of concern was the performance of the system during maximum backpressure conditions. In both axial and centrifugal compressors, the phenomenon of surge is encountered when the back-pressure is increased beyond peak levels. In some cases this surge can be violent and result in serious dynamic loads on the system. As a result, most compressor test programs include the investigation and definition of stability limits and the characterization of the stability of operation beyond these limits. In the case of supersonic flight inlets, when maximum allowable back-pressure levels are exceeded the shock system in the inlet can be completely destabilized and collapsed

resulting in a process often referred to as "un-start". Under certain conditions supersonic inlet un-start events can result in significant transient aerodynamic loads that often impact the overall design of the system.

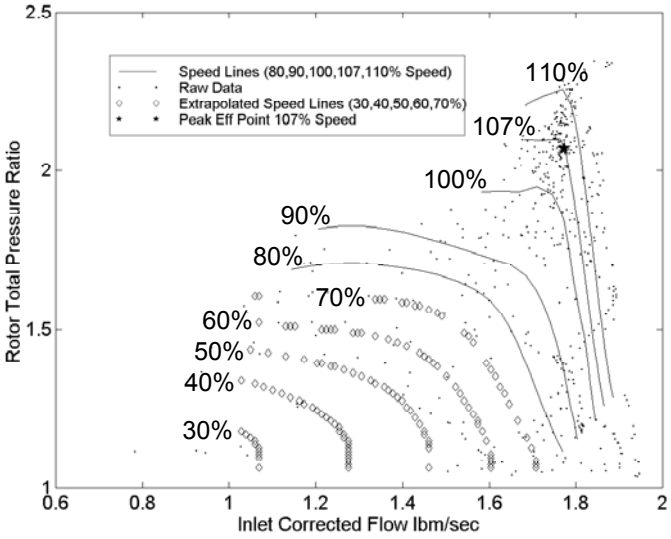

Figure 5. Compressor characteristics at various speeds

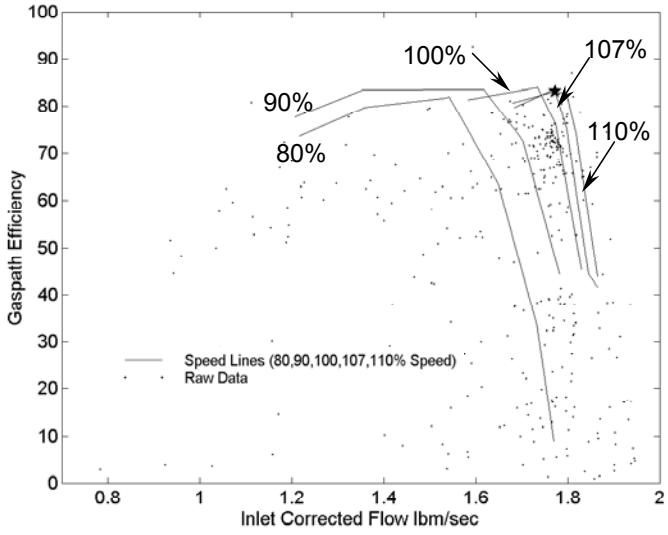

Figure 6. Rotor efficiency at various speeds

Thus, the stability of the supersonic rotor when operating at, and beyond peak compression levels received a significant amount of attention. The result of these tests was that the supersonic flow-paths in the rotor had very benign un-start characteristics. As the compression level was increased, the mass flow of the system remained nearly constant resulting in a largely vertical compressor characteristic. As the maximum compression levels were approached, mass flow would begin to drop off as the terminal normal shock was pushed upstream of the throat and onto the compression ramp. Once the normal shock progressed onto the ramp bleed holes on the ramp allowed an increase in bleed to account for the decreased ability of the flow-path throat to pass the captured mass flow. In this fashion the shock was pushed progressively farther toward the inlet capture plane as back-pressure was increased. This process occurred in a smooth and continuous process resulting in a continuous decrease in mass flow until finally, after a significant decrease in system mass flow, vibration levels would begin to increase owing to the fundamentally unstable nature of the completely un-started inlet flow-field.

The decrease in mass flow with increasing pressure is shown in Figure 5, which shows compressor characteristics at speeds ranging from 30% to 110%. These characteristics were generated with relatively tight tip clearances. The lower speed lines were extrapolated from limited data. Many other sensitivities and trade studies were performed but a complete presentation of the results is beyond the scope of this paper.

Figure 6 shows a plot of rotor-only, or gas-path, efficiency as a function of inlet corrected flow for a number of different rotor speeds. The efficiency levels shown here do not include the losses to the system due to the bleed gas removed from the flow-path or any other system losses – this plot shows adiabatic compression efficiency of the supersonic rotor gas-path only. The star on Figure 6 is a point indicating the peak efficiency achieved by the system during tests conducted to date.

The peak efficiency of any compressor is always an important feature but sometimes the "off-design" performance characteristics are just as important. As Figure 6 shows, the efficiency of the rotor does not drop-off significantly with decreased speed. This is important for systems that must spend a significant amount of time operating at less than 100% speed or pressure ratio.

To summarize test results to date, initial tests have shown that the stage starts and achieves good peak performance levels with potential for further improvement and optimization. The performance characteristics are consistent with the analytical models used to design the system.

Testing indicates that the stage has benign un-start or surge characteristics, a nearly vertical full speed compressor characteristic and promising off-design operating capability. Because of the high stage pressure ratio, the system performance is sensitive to tip gap. The lessons learned in the design and operation of this test rig are being applied to the design of a rig capable of operating at the increased speeds required to achieve the 9.9:1 pressure ratio.

4. REFRIGERATION COMPRESSION

The use of compressors of various types and sizes in refrigeration cycles is common practice. Using the design tools developed and validated by the recent rig tests using air as a working fluid, six refrigeration compressor design points were investigated and are summarized in Table 2. Cases one through four correspond to the compression levels that would be required for 500 ton water-cooled chiller systems that would operate on R134a, R410a, Ammonia and water respectively. Cases five and six are meant to represent the compression levels that would be applicable to smaller 3.5 ton air cooled AC units that might see use in smaller applications.

Also shown in Table 2 are a number of other thermodynamic properties that define the state of the gas at the compressor inflow and outflow stations. It should be noted that these gases are highly non-ideal and the property variations of the gas that occur throughout the compression process cannot be expected to obey the simplified relationships typically used to model the behavior of an ideal gas. The use of a supersonic shock compression stage was investigated for each of these cases. In order to address the non-ideal nature of these gases the NIST gas property program REFPROP 7.0 was used to predict the behavior of the various gasses as they underwent the shock compression processes.

Table 2 also summarizes the properties and conditions of the various refrigerants at the inflow and discharge of the compressor as well as a summary of compressor stage details. The results from the conceptual design study are summarized in the following sections on a case-by-case basis.

4.1 Case 1 (Fluid =R134a, PR=2.53)

This case corresponds to the requirements of a 500 ton water cooled chiller system. Because of the relatively low pressure ratio required for the proposed cycle, a relatively low inlet relative Mach number of ~1.39 is required. In order to process the proposed mass flow of refrigerant, the rotor would have a strake tip diameter of 37.44 cm and would operate at 9,800 rpm. Based on a set of assumptions for the loss levels of the various components of the compressor, an overall adiabatic compression efficiency of ~87.5% was predicted for this system, including the loss associated with the bleed required for shock stabilization. It is expected that in a production system, the bleed flow rate and energy recovery would be optimized to produce the highest system efficiency. For the purposes of this analysis, these conservative assumptions result in a drive power requirement of ~272 kW, neglecting any mechanical or electrical system losses and a kW/RT of ~0.5434.

4.2 Case 2 (Fluid=R410a, PR=2.28)

As with Case1, this compressor was intended to fit the requirements of a 500 ton water cooled chiller but because of the different thermodynamic properties of the R410a refrigerant, the rotor in this system would need to operate with an inlet relative Mach number of ~1.38. In order to process the proposed mass flow the rotor would need to have a strake tip diameter of 22.46 cm and would operate at a speed of 18,600 rpm. With the component loss levels assumed for this case, an overall adiabatic efficiency of ~87.9% was predicted for the system including an estimate for the associated shock bleed flow losses. This would result in a drive power requirement of ~299 kW, neglecting any mechanical or electrical system losses and a kW/RT of ~0.5976

4.3 Case 3 (Fluid=Ammonia, PR=2.61)

As with Case 1, this compressor was intended to fit the requirements of a 500 ton water cooled chiller but because of the properties of ammonia this system would need to operate with an inlet relative Mach number of ~1.46. In order to process the proposed mass flow the rotor would need to have a strake tip diameter of 16.6cm and would operate at a speed of 57,300 rpm. With the component loss levels assumed for this case, an overall adiabatic efficiency of

~84.0% was predicted for the system including an estimate for the associated shock bleed flow losses. This would result in a drive power requirement of ~259 kW, neglecting any mechanical or electrical system losses and a kW/RT of ~0.5170.

Table 2. Summary of design cases and inflow conditions

Property	Units	Case 1 (R134a)	Case 2 (R410a)	Case 3 (Ammonia)	Case 4 (Water)	Case 5 (R134a)	Case 6 (R410a)
Pressure Ratio		2.53	2.28	2.61	7.08	4.17	3.61
Mass Flow	kg/s	11.12	10.25	1.57	0.73	0.09	0.09
P_1	kPa	356.46	949.41	526.07	0.82	377.14	998.36
T_1	K	278.89	278.89	278.89	278.89	290.00	290.00
ρ_1	kg/m^3	17.4377	36.4564	4.1891	0.0064	17.5466	35.8830
h_1	kJ/kg	402.26	423.38	1612.69	2513.25	411.91	434.57
a_1	m/s	146.79	168.70	402.49	413.25	150.65	174.81
P_2	kPa	894.91	2357.01	1346.89	5.67	1547.29	3537.09
T_2	K	315.88	330.55	360.33	478.69	347.08	363.36
ρ_2	kg/m^3	41.8048	82.7493	8.2493	0.0256	69.3236	114.1740
h_2	kJ/kg	425.45	454.29	1782.86	2892.13	447.17	477.95
a_2	m/s	146.00	172.82	455.98	537.97	146.00	179.83
Rotor Speed	rpm	9,766	18,558	57,293	4,636	128,122	217,146
$\eta_{thermal}$	–	0.8854	0.8876	0.8492	0.8894	0.8738	0.8697
η_{stage}	–	0.8767	0.8787	0.8401	0.9126	0.8421	0.8368
Gas Power	kw	271.7	298.8	258.5	273.0	3.4	4.0
kW/RT		0.5434	0.5976	0.5170	0.5460	0.9714	1.1428

4.4 Case 4 (Fluid=Water Vapor, PR=7.08)

As with Case1, this compressor was intended to fit the requirements of a 500 ton water cooled chiller. The use of water vapor as a refrigerant in this case resulted in a low compressor supply pressure and density. The combination of the low density and relatively high pressure ratio resulted in a much larger wheel for this 5,664 m^3/min case. The inlet relative Mach number required to achieve the pressure ratio was ~ 2.07. In order to process the proposed mass flow the rotor would need to have a strake tip diameter of 255.2 cm and would operate at a speed of 4,636 rpm. With the component loss levels assumed for this case, an overall adiabatic efficiency of ~91.3% was predicted for the system including an estimate for the losses associated with the 4% boundary layer control and shock bleed flow. This would result in a drive power requirement of ~273 kW, neglecting any mechanical system losses and a kW/RT of 0.5460.

4.5 Cases 5 & 6

Cases five and six are meant to represent the compression levels that would be applicable to smaller 3.5 ton air cooled AC units that might see use in smaller applications. Both of these rotors were quite small and operated at high speeds. Manufacturing such small rotors would certainly present challenges. The high rotor speeds would either require significant gearing from a conventional motor or a direct drive system using a high-peed permanent magnet motor. See Table 2 for more mechanical and thermodynamic information on these two cases.

5. CONCLUSIONS

Preliminary rig testing has validated the design tools, performance capability and operational stability of an axial flow supersonic shock compression stage. The stage has been proposed for use in high pressure ratio air compressor applications. Recent work indicates that the stage may be applicable to the lower pressure ratio requirements often encountered in refrigeration systems.

Six conceptual refrigerant compression systems were evaluated as a basis for comparison to existing technology. The results of these conceptual design studies were presented. The compressor layouts for 500 ton water cooled chiller systems were evaluated using R134a, R410a, Ammonia and water vapor as refrigerants. The R134a, R410a and Ammonia systems all resulted in layouts that appear to be workable from a mechanical design perspective and achieve competitive efficiency levels.

The compressor layout for the 500 ton water cooled chiller system using water vapor as a refrigerant resulted in a rotor that was at the limit of practical application for the speed required to achieve the necessary compression level.

Compressors for two smaller 3.5 ton air cooled AC systems were also investigated. One system was designed for operation using R134a and the other for R410a. Both of these compressors ended up being quite small and operating at high speeds. Manufacturing such small rotors would certainly present challenges. The high rotor speeds would either require significant gearing from a conventional motor or direct drive system using a high-peed permanent magnet motor.

NOMENCLATURE

a	speed of sound	(m/s)
h	static enthalpy	(kJ/kg)
P	pressure	(kPa)
M	Mach number	(---)
T	temperature	(K)
γ	ratio of specific heats	(---)
η	efficiency	(---)
ρ	density	(kg/m^3)

Subscripts

axial	denotes axial direction
hub	hub of rotor
rel	denotes relative flow
stage	denotes overall stage
tan	denotes tangential direction
thermal	thermal efficiency – including bleed losses
tip	tip of rotor
ad	adiabatic
pt	total pressure
t	total condition
0	free stream condition
1	flow entering compressor
2	flow leaving compressor

REFERENCES

Billig, F., Van Wie, D., 1987, Efficiency parameters for inlets operating at hypersonic speeds, Eighth International Symposium on Air-Breathing Engines: p. 118-130.

Jacklitch, J., Hartmann, M., 1953, Investigation of 16-inch impulse-type supersonic compressor rotor with turning past axial direction, NACA RM E53D13.

Kantrowitz, A., 1948, The supersonic axial flow compressor, Langley Aeronautical Laboratory Report 974.

Kerrebrock, J., Drela, M., Merchant, A., Shuler, B., 1998, A family of designs for aspirated compressors, 98-GT-196.

Simon, H., 1973, A contribution to the theoretical and experimental examination of the flow through plane supersonic deceleration cascades and supersonic compressor rotors, Journal of Engineering for Power.

Wilcox, W., Tysl, E., Hartmann, M., 1959, Resume of the supersonic-compressor research at NACA Lewis Laboratory, Journal of Basic Engineering.

Wright, L., Klapproth, J., 1949, Performance of supersonic axial-flow compressors based on one dimensional analysis, NACA RM No. E8L10.

ACKNOWLEDGEMENT

This effort was funded in part by the Department of Energy under the cooperative agreement #DE-FC26 00NT40, awarded between the period of October 1, 2003 and September 30, 2004.